Theory of Enhanced Reversed Shear Mode in Tokamaks

K. C. Shaing and A. Y. Aydemir
Institute for Fusion Studies, The University of Texas at Austin, Austin, Texas 78712

W. A. Houlberg
Fusion Energy Division, ORNL, P.O. Box 2009, Oak Ridge, Tennessee 37831-8071

M. C. Zarnstorff
Princeton Plasma Physics Laboratory, P.O. Box 451, Princeton, New Jersey 08543
(Received 11 March 1998)

It is shown that toroidal-magnetic-field ripple-induced particle flux can drive poloidal $\boldsymbol{E} \times \boldsymbol{B}$ speed to bifurcate over the local maximum of the nonlinear poloidal (or parallel) viscosity. Here, $\boldsymbol{E}$ is the electric field, and $\boldsymbol{B}$ is the magnetic field. This mechanism, together with the turbulence suppression due to the radial gradient of the $\boldsymbol{E} \times \boldsymbol{B}$ and diamagnetic angular velocity, is employed to explain the enhanced reversed shear mode observed in the core region of tokamaks. [S0031-9007(98)06348-0]

PACS numbers: 52.55.Fa, 52.25.Fi

An improved plasma confinement regime (H mode) has been observed in the edge region of many tokamaks and stellarators [1–6]. It is initiated by a sudden increase in the magnitude of the poloidal $\boldsymbol{E} \times \boldsymbol{B}$ speed and followed by the turbulence suppression which leads to better plasma confinement [2,4]. Here $\boldsymbol{E}$ is the electric field, and $\boldsymbol{B}$ is the magnetic field. A quantitative theory based on the bifurcation of the poloidal $\boldsymbol{E} \times \boldsymbol{B}$ Mach number $U_{\rm pm}$ over the local maximum of the nonlinear plasma viscosity and the subsequent turbulence suppression due to the radial gradient of the $\boldsymbol{E} \times \boldsymbol{B}$ and diamagnetic angular velocity is in good agreement with both electrode induced and naturally occurring H modes [7,8]. Here, we extend the H-mode theory to explain the improved plasma confinement regime—enhanced reverse shear (ERS) mode—in the core region [9,10]. Indeed, it is observed in Tokamak Fusion Test Reactor (TFTR) that there is a sudden jump in the radial electric field prior to the onset of the ERS mode [11]. The corresponding value of $U_{\rm pm}$ is greater than unity. This phenomenon is the same as that in the H mode. Furthermore, because the slope of the radial electric field changes sign in the bifurcation layer, the appropriate bifurcation quantity is the radial electric field and not the gradient of the radial electric field. Confinement improvement theory based on the bifurcation of $U_{\rm pm}$ is consistent with this observation.

It is obvious that the ion orbit loss mechanism which is responsible for the bifurcation of the poloidal $\boldsymbol{E} \times \boldsymbol{B}$ speed in the naturally occurring H mode is not effective in the core region because the number of particles that intersect the plasma boundary is small. One therefore has to find a different mechanism to drive $U_{\rm pm} \equiv V_{\|i}/v_{ti} - cE_r/v_{ti}B_p$ over the local maximum of the parallel (or poloidal) viscosity. Here, $V_{\|i}$ is the ion parallel flow, c is the speed of light, E_r is the radial electric field, B_p is the poloidal magnetic field strength, and v_{ti} is the ion thermal speed. There are such mechanisms. One possible mechanism is the momentum input associated with the injected neutral particle beam. The other is the toroidal-magnetic-field ripple-induced particle flux. Because an enhanced reversed shear mode exists even in the balanced neutral particle beam injection operations, we focus on the bifurcation of $U_{\rm pm}$ driven by the ripple-induced particle flux. Note that ripple-trapped particle flux can drive bifurcation has already been demonstrated in Refs. [12,13]. In Ref. [12], it is shown that electron $1/\nu$ flux can cause a radial electric field to bifurcate to a more positive value. In Ref. [13], ion $1/\nu$ flux is used to drive the radial electric field to bifurcation in the stellarator H-mode theory.

There are two types of ripple-induced particle flux. One is due to ripple trapping [14]. In the relatively collisional regime, it contributes to the $1/\nu$ flux [15]. The other is due to the modification of the trajectories of the toroidally trapped particles (i.e., bananas) and barely toroidally trapped or circulating particles by the magnetic field ripple. This class of orbits is not trapped in the ripple well. In the low collisionality regime, it contributes to the stochastic ripple plateau flux [16,17]. The constitutive relations between ripple-induced particle flux and the components of the viscous tensor are adequately understood. We employ these constitutive relations in a momentum equation.

The momentum equation is

$$\sum_a n_a m_a \frac{d\boldsymbol{V}_a}{dt} = \frac{1}{c}\boldsymbol{J} \times \boldsymbol{B} - \nabla\left(\sum_a p_a\right) - \nabla \cdot \left(\sum_a \boldsymbol{\pi}_a\right) + \left(\sum_a \boldsymbol{S}_{\rm ma} - \sum_a m_a \boldsymbol{V}_a S_{\rm na}\right), \quad (1)$$

where the subscript a indicates the plasma species, n_a is the plasma density, m_a is the mass, $\boldsymbol{V}_a$ is the flow velocity, $\boldsymbol{J}$ is the plasma current, p_a is the plasma pressure, $\boldsymbol{\pi}_a$ is

 © 1998 The American Physical Society

the viscous tensor, $\boldsymbol{S}_{\rm ma}$ is the momentum source, and $S_{\rm na}$ is the particle source. Note that the particle source associated with gas puffing or pellet injection reduces velocity. The d/dt operator in Eq. (1) is $d/dt = \partial/\partial t + \boldsymbol{V}_a \cdot \nabla$. The steady state parallel component of Eq. (1) is

$$\left\langle \boldsymbol{B} \cdot \nabla \cdot \sum_a \boldsymbol{\pi}_a \right\rangle = \left\langle \boldsymbol{B} \cdot \sum_a \boldsymbol{S}_{\rm ma} \right\rangle - \left\langle \boldsymbol{B} \cdot \sum_a m_a \boldsymbol{V}_a S_{\rm na} \right\rangle, \quad (2)$$

where the angular brackets denote flux surface averaging. Because we are interested in the case where $U_{\rm pm} \sim 1$ but $|\boldsymbol{V}_a|/v_{\rm ta} < 1$, the convective term $\boldsymbol{V}_a \cdot \nabla \boldsymbol{V}_a$ can be neglected. Here, v_{ta} is the thermal speed of species a. The steady state toroidal component of Eq. (1) is

$$\left\langle \boldsymbol{B}_t \cdot \nabla \cdot \sum_a \boldsymbol{\pi}_a \right\rangle = \left\langle \boldsymbol{B}_t \cdot \sum_a \boldsymbol{S}_{\rm ma} \right\rangle - \left\langle \boldsymbol{B}_t \cdot \sum_a m_a \boldsymbol{V}_a S_{\rm na} \right\rangle. \quad (3)$$

We employ here Hamada coordinates: $\boldsymbol{B} = \boldsymbol{B}_t + \boldsymbol{B}_p = \psi' \nabla V \times \nabla\theta - \chi' \nabla V \times \nabla\zeta$, where $\boldsymbol{B}_t$ is the toroidal magnetic field, $\boldsymbol{B}_p$ is the poloidal magnetic field, $\psi' = \boldsymbol{B} \cdot \nabla\zeta$, $\chi' = \boldsymbol{B} \cdot \nabla\theta$, θ is the poloidal angle, ζ is the toroidal angle, and V is the volume enclosed in the flux surface [18]. Note that $\langle \boldsymbol{B}_t \cdot \boldsymbol{J} \times \boldsymbol{B} \rangle$ is related to $\partial \langle \boldsymbol{E} \cdot \nabla V \rangle / \partial t$ through Ampère's law and vanishes at steady state. Equations (2) and (3) completely determine the flow velocity $\boldsymbol{V}_a$ within the flux surface. To the leading order of gyroradius expansion $\boldsymbol{V}_a = V_{\|a} \hat{n} + \boldsymbol{V}_{\perp a}$, and $\boldsymbol{V}_{\perp a} = c\boldsymbol{B} \times \nabla\Phi/B^2 + c\boldsymbol{B} \times \nabla p_a / n_a e_a B^2$, where $\hat{n} = \boldsymbol{B}/B$, Φ is the electrostatic potential, and e_a is the electric charge. Because $\Phi = \Phi(V)$ and $p_a = p_a(V)$, $\boldsymbol{V}_a \cdot \nabla V = 0$. Thus, there are two unknowns: parallel flow $V_{\|a}$ and $\nabla\Phi \cdot \nabla V$ to be determined from Eqs. (2) and (3). For simplicity, we consider only electron-ion plasmas. Because electron friction is much larger than electron viscous force in large aspect ratio tokamaks, $V_{\|i} \approx V_{\|e}$ to the leading order of the ratio of electron viscous force to the electron friction force.

From the general expressions for the plasma viscosity in the plateau regime, we can evaluate ripple plateau viscosity for a model rippled tokamak $B = B_0(1 - \epsilon \cos\theta - \delta \cos N\zeta)$, where B_0 is B on the magnetic axis, N is the number of toroidal magnetic field coils, ϵ is the inverse aspect ratio, and δ is the ripple amplitude to obtain [19]

$$\begin{aligned} \langle \boldsymbol{B}_t \cdot \nabla \cdot \boldsymbol{\pi}_a \rangle_{rp} &= \langle \boldsymbol{B} \cdot \nabla \cdot \boldsymbol{\pi}_a \rangle_{rp} \\ &= \frac{\sqrt{\pi}}{4} n_a m_a \frac{v_{ta}^2}{Rq} C_1 B_0 (Nq\delta^2) \left(\frac{B_p^2}{B}\right)^2 \\ &\quad \times \left\{ \frac{V_{\|a}}{v_{ta}} \left(\frac{B}{B_p}\right)^2 + \left(\frac{cE_r}{B_p v_{ta}} - \frac{cp_a'}{neB_p v_{ta}} \right) + \frac{1}{5} \left[\frac{q_{\|a}}{p_a v_{ta}} \left(\frac{B}{B_p}\right)^2 - \frac{5}{2} \frac{cT_a'}{e_a B_p v_{ta}} \right] \right\}, \end{aligned} \quad (4)$$

where prime denotes d/dr, R is the major radius, r is the local minor radius, $C_1 = 2$, q is the safety factor, $q_{\|a}$ is the parallel heat flow, T_a is the temperature, and subscript rp indicates the ripple plateau regime. We have approximated Hamada coordinates with cylindrical coordinates in Eq. (4). Note that electron ripple plateau viscosity is much smaller than that of ions and can be neglected. Because we are interested in the case $U_{\rm pm} \sim 1$ and $B_p/B \ll 1$, we conclude ripple plateau viscosity mainly damps toroidal flow. Indeed, for $T_i = 5$ keV, $R = 2.6$ m, $q = 2.5$, $N = 20$, and $\delta = 1.3 \times 10^{-3}$, the toroidal momentum damping time τ_M is $\tau_M^{-1} = (\sqrt{\pi}/2) C_1 (v_{ti}/Rq)(Nq\delta^2/2) \simeq 11.6\ {\rm s}^{-1}$ or $\tau_M = 0.086$ s. Because this damping time is much shorter than the diffusive neoclassical toroidal viscosity [20], we neglect the latter contribution here. Note that the contribution from the $\epsilon \cos\theta$ variation of B to $\langle \boldsymbol{B} \cdot \nabla \cdot \boldsymbol{\pi} \rangle$ is ignored in Eq. (4) because we assume that toroidally trapped particles are in the banana regime which contributes to the nonlinear viscosity.

Ripple trapping induced particle flux has several collisionality regimes. Here, we only employ the $1/\nu$ flux $\Gamma_{1/\nu}$ calculated in Refs. [15,21] to demonstrate the fundamental bifurcation physics. The corresponding viscosity is [13]

$$\begin{aligned} \langle \boldsymbol{B}_p \cdot \nabla \cdot \boldsymbol{\pi}_i \rangle_{1/\nu} &= -\langle \boldsymbol{B}_t \cdot \nabla \cdot \boldsymbol{\pi}_i \rangle_{1/\nu} = -\frac{e}{c} B_p B \Gamma_{1/\nu} \\ &= -\frac{64 G(\alpha)}{9(2\pi)^{3/2}} n_i \epsilon^2 \delta^{3/2} \left(\frac{cT_i}{eBr}\right)^2 \frac{27.4}{\nu_i} \left[\left(\frac{p_i'}{p_i} - \frac{eE_r}{T_i} \right) + 2.37 \frac{T_i'}{T_i} \right] \left(\frac{eBB_p}{c} \right), \end{aligned} \quad (5)$$

where $\alpha = \epsilon/(Nq\delta)$, and ν_i is ion-ion-collison frequency. Note that $G(\alpha)$ is a function that accounts for the variation of the local ripple well depth, and, for $\alpha \gg 1$, $G(\alpha) \simeq 0.02/\alpha^3$ [15]. It is obvious from Eq. (5) $\langle \boldsymbol{B} \cdot \nabla \cdot \boldsymbol{\pi}_i \rangle_{1/\nu} = 0$. Because electron $1/\nu$ flux is smaller than that of ions, it is neglected.

The nonlinear resonant plasma viscosity due to banana and circulating particles is [22,23]

$$\langle \boldsymbol{B} \cdot \nabla \cdot \boldsymbol{\pi} \rangle_n = n_a m_a B^2 \left(\mu_{1a} U_{\theta a} + \frac{2}{5} \mu_{2a} \frac{q_{\theta a}}{p_a} \right), \quad (6)$$

where the subscript n indicates nonlinear viscosity, $U_{\theta a} = (v_{ta}/B)[V_{\|a}/v_{ta} - cE_r/(B_p v_{ta}) + cp_a'/(n_a e_a v_{ta} B_p)]$,

and $q_{\theta a}/p_a = (v_{ta}/B)[q_{\|a}/(p_a v_{ta}) + \frac{5}{2} c T_a'/(e_a v_{ta} B_p)]$. Because $V_{\|e} \approx V_{\|i} \ll v_{te}$, and $cE_r/(B_p v_{te}) \ll 1$, electron viscosity is not affected in the regime where $U_{\rm pm} \sim 1$, standard electron viscosity coefficients [24] apply. The ion nonlinear resonant viscosity coefficients are [22,23] $(\mu_{1i}, \mu_{2i}) = \int_{|U_{\rm pm}|}^{\infty} dx\, x^4 e^{-x^2} [(\kappa_B \kappa_{\rm ps})/(\kappa_B + \kappa_{\rm ps})](1, x^2 - \frac{5}{2})$, where $\kappa_{\rm ps}(x) = (\nu_i e^2/2\sqrt{\pi}) \times \int_{-1}^{1} dy (1 - 3y^2)(\nu_* x/\nu_i) \times \{(y + U_{\rm pm}/x)^2 + [\nu_* \times \epsilon^{3/2} \nu_T(x)/\nu_i x]^2\}^{-1}$, $\nu_* = \nu_i R q/(\epsilon^{3/2} v_{ti})$, $\nu_T = 3\nu_D(x) + \nu_E(x)$ is the anisotropy relaxation frequency, $\kappa_B(x) = 1.46\sqrt{\epsilon}\, \nu_D (8/3\sqrt{\pi})(1 - 3U_{\rm pm}^2/x^2)\mathbb{F}(1 + U_{\rm pm}^2/x^2)^{-3/2}$, $\mathbb{F} = (1 - U_{\rm pm}^2/x^2) + (\nu_\|/\nu_D) U_{\rm pm}^2/x^2$, ν_D, ν_E, and $\nu_\|$ are defined in Ref. [24]. In the limit of $|U_{\rm pm}| \to 0$, Eq. (6) reproduces standard viscosity coefficients that connect smoothly all collisionality regimes.

The nonlinearity in Eqs. (2) and (3) is in nonlinear viscosity shown in Eq. (6). Because of this nonlinearity, $U_{\rm pm}$ can have bifurcated solutions. To show this, for simplicity, we assumed particle source $S_{\rm na}$ vanishes. The momentum source can be eliminated by assuming $\langle \boldsymbol{B} \cdot \sum_a \boldsymbol{S}_{\rm ma} \rangle \approx \langle \boldsymbol{B}_t \cdot \sum_a \boldsymbol{S}_{\rm ma} \rangle$ and subtracting Eq. (3) from Eq. (2) to obtain

$$\left\langle \boldsymbol{B}_p \cdot \nabla \cdot \sum_a \boldsymbol{\pi}_a \right\rangle = 0\,, \tag{7}$$

which is basically the poloidal momentum balance equation. Because $\langle \boldsymbol{B} \cdot \nabla \cdot \boldsymbol{\pi}_a \rangle_n = \langle \boldsymbol{B}_p \cdot \nabla \cdot \boldsymbol{\pi}_a \rangle_n$ in Hamada coordinates, the explicit expression for Eq. (7) is $\langle \boldsymbol{B}_p \cdot \nabla \cdot \sum_a \boldsymbol{\pi}_a \rangle_n + \langle \boldsymbol{B}_p \cdot \nabla \cdot \sum_a \boldsymbol{\pi}_a \rangle_{1/\nu} = 0$. Substituting Eqs. (5) and (6) into (7), we obtain a dimensionless bifurcation equation:

$$\frac{M_i \mu_{1i}}{M_e \mu_{1e}} (U_{\rm pm} - \overline{A}) = -U_{\rm pm} - \overline{B} - \frac{1}{Nq} \frac{32 G(\alpha)}{9(2\pi)^{3/2}} \frac{1}{\nu_{*e} \nu_{*\delta}} \left(\frac{\nu_e \sqrt{\epsilon}}{\mu_{1e}} \right) \left(\frac{T_i M_i}{T_e M_e} \right)^{1/2} \left[27.4 \left(U_{\rm pm} - \frac{V_{\|i}}{v_{ti}} - \overline{C} \right) \right], \tag{8}$$

where $\nu_{*e} = \nu_e R q/(v_{te} \epsilon^{3/2})$, ν_e is the electron-electron collision frequency, $\nu_{*\delta} = \nu_i R/(v_{ti} N \delta^{3/2})$, $\overline{A} = -[c/(e v_{ti} B_p)](p_i'/n_i + \mu_{2i} T_i'/\mu_{1i})$, $\overline{B} = -[c/(e v_{ti} B_p)] \times (p_e'/n_i + \mu_{2e} T_e'/\mu_{1e})$, and $\overline{C} = -[c/(e B_p v_{ti})] \times (p_i'/n_i + 2.37 T_i')$. Parallel heat flows are ignored in Eq. (8) because heat frictions are larger than heat viscosities in a large aspect ratio tokamak and to the leading order $q_{\|i} \approx q_{\|e} \approx 0$. Note that $(V_{\|i}/v_{ti})$ in Eq. (8) denotes the coupling between Eq. (8) and Eq. (3). However, because $|U_{\rm pm}| \sim 1$ and $|V_{\|i}/v_{ti}| < 1$, we ignore $(V_{\|i}/v_{ti})$ in Eq. (8) and thus decouple Eqs. (3) and (8).

Equation (8) is a nonlinear equation for $U_{\rm pm}$. The solution is found graphically by plotting the right side and left side of the equation versus $U_{\rm pm}$ as shown in Figs. 1–3. The parameters used are $n_e = 3 \times 10^{19}$ cm^{-3}, $\overline{A} = \overline{B} = 0.2$, $T_e = 5.5$ keV, $B = 4.6$ T, $R = 2.6$ m, $a = 0.8$ m, $\epsilon = 0.1$, $N = 20$, $q = 2.5$, $\delta = 1.3 \times 10^{-3}$, and $V_{\|i}/v_{ti} = 0$. In Fig. 1, for $T_i = 5.5$ keV and $\overline{C} = 0.8$, there is only one solution, and $U_{\rm pm} < 1$. This is the conventional solution. As $\overline{C}$ and T_i increase to $\overline{C} = 2.75$ and $T_i = 6.5$ keV, there can be three solutions as shown in Fig. 2. One of the new solutions, the one in the middle, is unstable. The other stable new solution is in the $U_{\rm pm} > 1$ regime. When $\overline{C}$ and T_i increase further to $\overline{C} = 3.0$ and $T_i = 7.5$ keV, the conventional solution disappears, and only the stable $U_{\rm pm} > 1$ solution exists. Note that the most effective way to increase $\overline{C}$ is to increase the ion temperature gradient because the numerical coefficient in front of dT_i/dr is larger than that of dn_e/dr. When the heating power increases, both T_i and $\overline{C}$ increase. As T_i and $\overline{C}$ increase, $U_{\rm pm}$ increases and eventually bifurcates from $U_{\rm pm} < 1$ to $U_{\rm pm} > 1$ regime. This sudden increase of $U_{\rm pm}$ is similar to the observed abrupt jump of E_r in the ERS mode in TFTR. The bifurcated value of $U_{\rm pm}$ is about 2 in this example. The observed $U_{\rm pm}$ is greater than unity [11].

After bifurcation, the turbulence fluctuation level is reduced by a factor of $1/[1 + \kappa(\omega')^2]$, where ω' is the radial

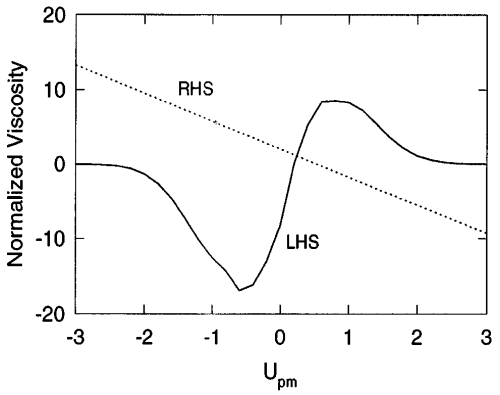

FIG. 1. Right-hand side (RHS) and left-hand side (LHS) of Eq. (8) versus $U_{\rm pm}$. There is one solution which corresponds to the conventional confinement mode.

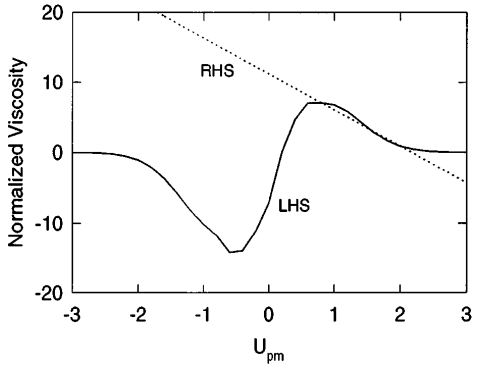

FIG. 2. As T_i and $\overline{C}$ increase, the value of $U_{\rm pm}$ increases. Here, there are three solutions. The one in the middle is unstable. The solution with the largest value of $U_{\rm pm}$ is the new stable solution, which corresponds to the ERS mode.

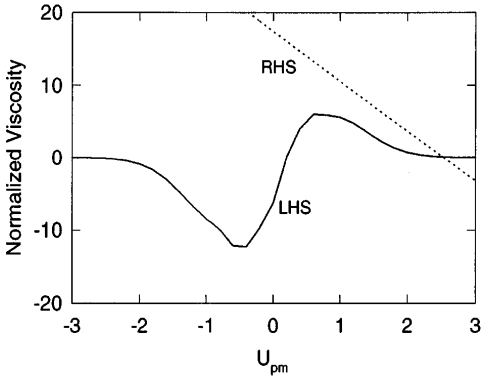

FIG. 3. When T_i and $\overline{C}$ increase further, only the ERS mode solution exists.

gradient of the $\boldsymbol{E} \times \boldsymbol{B}$ and diamagnetic angular velocity, κ is a normalization constant, and plasma confinement improves [25–27].

The fact that magnetic shear is reversed is not employed explicitly in the theory. It could be that reversed magnetic shear stabilizes magnetohydrodynamics (MHD) activities, such as sawteeth, and therefore reduces magnetic stress associated with the perturbed $\boldsymbol{J} \times \boldsymbol{B}$ force. Magnetic stress increases nonambipolar electron loss and may prevent bifurcation of $U_{\rm pm}$. It could also be that turbulence fluctuation levels are lower inside the $q_{\rm min}$ radius [28], therefore it is easier to increase T_i and dT_i/dr with heating power inside the $q_{\rm min}$ radius, which in turn facilitates the bifurcation. Here $q_{\rm min}$ is the minimum value of q.

The plasma parameters in Figs. 1–3 are at the tail end of the $1/\nu$ regime. If T_i increases further, ripple trapping viscosity will move into the ν regime [14], and its magnitude will decrease as ν decreases. This is the likely cause for the ultimate relaxation of $U_{\rm pm}$. The other possible cause is the magnetic stress associated with the MHD activity observed after bifurcation. The effect of neutral change exchange momentum loss [29] on the value of $U_{\rm pm}$ can be important because, for high temperature plasmas, nonlinear viscosity is weak. These issues will be addressed separately.

In summary, we develop a theory for enhanced reversed shear mode [30]. The physical process is as follows: (i) Reversed magnetic shear stabilizes MHD activities which reduces magnetic stress and reduces the turbulence fluctuations inside the $q_{\rm min}$ radius; (ii) when the heating power increases, both T_i and dT_i/dr increase. This leads to bifurcation of $U_{\rm pm}$; (iii) after $U_{\rm pm}$ bifurcation, the turbulence fluctuation level reduces by a factor of $1/[1 + \kappa(\omega')^2]$; (iv) evolution of the plasma profiles relaxes $U_{\rm pm}$; (v) however, $(\omega')^2$ is still substantial to suppress turbulence fluctuations and improve plasma confinement.

The authors thank R. E. Bell for many stimulating discussions. This work was supported by the U.S. Department of Energy Contract No. DE-FG03-96ER-54346.

[1] ASDEX Team, Nucl. Fusion **29**, 1959 (1989).
[2] R. J. Taylor, M. L. Brown, B. D. Fried, H. Grote, J. R. Liberati, G. J. Morales, and P. Pribyl, Phys. Rev. Lett. **63**, 2365 (1989).
[3] R. J. Groebner *et al.*, Phys. Rev. Lett. **64**, 3015 (1990).
[4] K. Ida *et al.*, Phys. Rev. Lett. **65**, 1364 (1990).
[5] F. Wagner *et al.*, Plasma Phys. Controlled Fusion **36**, A61 (1994).
[6] K. Toi *et al.*, in *Plasma Physics and Controlled Nuclear Fusion Research 1994* (International Atomic Energy Agency, Vienna, 1994), Vol. 2, p. 331.
[7] K. C. Shaing and E. C. Crume, Jr., Phys. Rev. Lett. **63**, 2369 (1989).
[8] S.-I. Itoh and K. Itoh, Phys. Rev. Lett. **60**, 2276 (1988).
[9] F. M. Levinton, M. C. Zarnstorff, S. H. Bartha, M. Bell, R. E. Bell, R. V. Budny, C. E. Bush, Z. Chang, E. D. Fredrickson, A. Janos, J. Manickam, S. T. Ramsey, G. L. Schmidt, E. J. Synakowski, and G. Taylor, Phys. Rev. Lett. **75**, 4417 (1995).
[10] S. Ishida *et al.*, Phys. Rev. Lett. **79**, 3917 (1997).
[11] R. E. Bell, Bull. Am. Phys. Soc. **42**, 1945 (1997); (to be published).
[12] K. Itoh and S.-I. Itoh, Nucl. Fusion **32**, 2243 (1992).
[13] K. C. Shaing, Phys. Rev. Lett. **76**, 4364 (1996).
[14] P. N. Yushmanov, Nucl. Fusion **22**, 315 (1982).
[15] J. W. Connor and R. J. Hastie, Nucl. Fusion **13**, 221 (1973).
[16] A. H. Boozer, Phys. Fluids **23**, 2282 (1980).
[17] R. J. Goldston, R. B. White, and A. H. Boozer, Phys. Rev. Lett. **47**, 647 (1981).
[18] S. Hamada, Prog. Theor. Phys. **22**, 145 (1959).
[19] K. C. Shaing, S. P. Hirshman, and J. D. Callen, Phys. Fluids **29**, 521 (1986). The reason ripple plateau flux is shown here is to illustrate the two-dimensional nature of the momentum equation to be solved.
[20] M. N. Rosenbluth *et al.*, in *Plasma Physics and Controlled Nuclear Fusion Research 1970* (International Atomic Energy Agency, Vienna, 1971), Vol. 1, p. 495.
[21] T. E. Stringer, Nucl. Fusion **16**, 12 (1972).
[22] K. C. Shaing, C. T. Hsu, and N. Dominguez, Phys. Plasmas **1**, 1168 (1994).
[23] K. C. Shaing, Phys. Fluids B **2**, 2847 (1990).
[24] S. P. Hirshman and D. J. Sigmar, Nucl. Fusion **21**, 1079 (1981).
[25] K. C. Shaing *et al.*, in *Plasma Physics and Controlled Nuclear Fusion Research 1988* (International Atomic Energy Agency, Vienna, 1989), Vol. 2, p. 13; K. C. Shaing, E. C. Crume, Jr., and W. A. Houlberg, Phys. Fluids B **2**, 1496 (1990).
[26] K. Itoh *et al.*, Plasma Phys. Controlled Fusion **36**, 123 (1994).
[27] Y. Z. Zhang and S. M. Mahajan, Phys. Fluids B **4**, 1385 (1992).
[28] K. Kishimoto *et al.*, in *Fusion Energy* (International Atomic Energy Agency, Vienna, 1996), Vol. 2, p. 581.
[29] M. Coronado and J. N. Talmadge, Phys. Fluids B **5**, 1200 (1993).
[30] Whether this theory is applicable to the negative central shear mode observed in DIII-D [E. J. Strait *et al.*, Phys. Rev. Lett. **75**, 4421 (1995)] remains to be seen.